

Performance Evaluation of Photovoltaic, Wind Turbine, and Concentrated Solar Power Systems in Morocco

El Baqqal Youssef*[‡] and Ferfra Mohamed**[‡]

* Department of Electrical Engineering, Mohammadia School of Engineers, Mohammed V University in Rabat, Ibn Sina Street P.B 765, Rabat, Morocco

** Department of Electrical Engineering, Mohammadia School of Engineers, Mohammed V University in Rabat, Ibn Sina Street P.B 765, Rabat, Morocco

(Youssef.elbaqqal@um5r.ac.ma, ferfra@emi.ac.ma)

[‡] El Baqqal Youssef; Ferfra Mohammed, Ibn Sina Street P.B 765, Rabat; Morocco

Tel: +212 661 064 792, Youssef.elbaqqal@um5r.ac.ma

Received: 06.07.2023 Accepted: 03.09.2024

Abstract- This paper presents an analysis of wind and solar energy production in three different locations in Morocco: Midelt, Dakhla, and Laayoune. Predictive models from existing literature are utilized to estimate energy production for photovoltaic (PV), concentrated solar power (CSP), and wind systems, along with the estimation of annual energy generation and capacity factor. Meteorological data collected from the System Advisor Model (SAM) software is used for each site in the analysis. To validate the results, a comparison is made with SAM's estimates, a widely recognized tool for evaluating renewable energy systems. The findings indicate a high solar potential in Dakhla, Midelt, and Laayoune, with capacity factors of PV plants ranging from 22.56% to 23.90%. CSP technology exhibits significant energy generation potential in all three locations. In terms of wind energy, Dakhla and Laayoune demonstrate superior wind turbine performance compared to Midelt, making them favorable locations for wind energy generation. Among the three locations, Laayoune stands out with the highest capacity factors and annual energy generation, making it the most suitable location for wind turbine deployment. Based on these findings, it is recommended to consider the integration of both solar and wind systems in Dakhla and Laayoune, taking advantage of their high potential for both energy sources. Such hybrid systems can contribute to stable energy production and cost reduction. Moreover, the simplicity and reliability of the models used in this study make them suitable for estimating energy production in such hybrid systems.

Keywords Renewable Energy; Wind Energy; Solar Photovoltaic; Concentrated Solar Power; Capacity Factor.

Nomenclature

A_{module}	Active area of each individual pv module	G_b	hourly beam solar radiation
A_r	Rotor area	G_d	hourly diffuse solar radiation
A_{sf}	Solar field area	$G_{noct.ref}$	Nominal solar radiation
C_f	Capacity factor	G_r	hourly Reflected solar radiation
Cl	Mean cleanliness factor	G_t	hourly global solar radiation
$\cos(\theta_{csp})$	Cos-loss efficiency	h	Hub Height
C_p	Power coefficient	h_a	Solar hour angle
E_{annual}	Annual electrical energy production	LST	Local standard time
f_{losses}	Derating factor	N_{module}	Total number

$P_{DC,peak,i}$	Peak power output of the PV plant	$P_{CSP,absorbed}$	Absorbed energy
P_{Losses}	Thermal losses	η_{IAM}	Incidence angle modifier-loss efficiency
P_{incid}	Total absorbed power	η_{PB}	Overall power block efficiency
P_{rated}	Rated electrical power	$\eta_{SF,therm}$	Solar field thermal efficiency
$P_{thermal}$	Available thermal energy	η_{SF}	Overall efficiency of CSP field
$P_{CSP,elec}$	Net electrical power	$\eta_{endlosses}$	Shadow-loss efficiency
$P_{CSP,thermal}$	Useful thermal output	η_{gen}	General error
$P_{DC,peak,i}$	Peak power output	$\eta_{generator}$	Nominal generator efficiency
P_{Losses}	Thermal losses	η_{geo}	Geometry effect efficiency
T_C	PV panel Temperature	$\eta_{inverter}$	Efficiency of the inverter
T_{amb}	Ambient temperature	η_{pv}	Actual efficiency
$T_{noct,ref}$	Nominal operating cell temperature,	$\eta_{pv,i}$	Efficiency
U_{lnoct}	Heat transfer factor	η_{ref}	Nominal efficiency
V_{ws}	Wind speed	η_{shadow}	End-loss efficiency
α	Wind shear	$\eta_{storage}$	Storage efficiency,
α_s	Solar altitude angle	η_{track}	Tracking error
β	Inclination angle	η_{turb}	Constant thermodynamic efficiency
γ	Solar azimuth angle	θ_{Csp}	Incidence angle
γ_s	Azimuth of the surface	θ_{pv}	Solar incidence angle of pv module
γ_t	Temperature factor	θ_z	Zenith angle
δ	Solar declination	λ	Longitude

1. introduction

Currently, Renewable energies have gained significant global attention and importance as the world progressively recognizes the urgent need to transition from fossil fuels to sustainable and clean energy sources. As a result, renewable energy sources, particularly wind and solar energies, are playing a major role in generating electrical energy and their contribution to the global energy mix continues to rise[1].

Over the past few decades, there has been remarkable global advancement in renewable energies field. Various renewable sources, such as wind power, solar photovoltaic (PV) systems, and concentrated solar power (CSP), have reached a significant level of technological maturity, making them more competitive in the energy market[2]. Moreover, the utilization of PV panels for electricity generation has witnessed a steady rise in recent years[3].

In 2021, the world saw an impressive increase in renewable energy generation, with approximately 257 GW added. This pushed the total global capacity to 3 064 GW[4]. Interestingly, solar and wind energy played an equally significant role in this growth, contributing 849 GW and 825 GW of capacity, respectively.

In this regard, the Moroccan government adopted an energy strategy based essentially on renewable energies. It outlines a plan for transitioning towards cleaner energy sources over the coming years, intending to raise the proportion of renewable energy in the country's electricity

supply to over 52% by 2030[5]. Precisely, the objective of this strategy is to attain 4.20 GW of wind and 4.56 GW of solar installed capacity excepting to reach, both, 40% of the total electrical capacity[6]. To do so, several renewable energy projects are being implemented in several locations in Morocco, especially wind and solar projects[7]. Consequently, notable progress in this pursuit over time has been made. Figure 1 presents the evolution of wind and solar installed capacity, as well as the renewable energy share of electricity capacity, from 2012 to 2021[4]. By the end of 2021, it is evident that the renewable energy portion of electricity capacity has reached 29.9%. This is a significant increase from the 23.8 % that was reported in 2012. Furthermore, it's apparent that, for wind capacity, this evolution is important growing from 291 MW installed by 2012 to 1435 by the end of 2021, in other words, the wind capacity has been developed five times during this period. There was a steady growth in solar installed capacity in Morocco between 2012 and 2021, with the most significant increase occurring in 2018, due to the completion of the CSP complex NOOR Ouarzazate.

In this particular context, numerous studies available in the literature provide descriptions and discussions regarding the evolution of renewable energy in Morocco[6][8]. Moreover, there is an evaluation of energy production and an analysis conducted on the efficiency of solar[9][10] and wind systems [11].

Fig 1. Growth of Wind and Solar Installed Capacity in Morocco

Hybrid energy systems, combining multiple sources, have become prevalent because renewable energy sources are often intermittent. Hybrid systems commonly utilize both wind and solar energy sources because they complement each other effectively[12]. Usually, this strategy proves to be more economical, effective, and dependable when contrasted with single-source systems [13]. It's regarded as one of the viable solutions to increase the reliability of the system[14]. Furthermore, it's acknowledged as important approach addressing present energy and environmental issues [15]. Nevertheless, implementing a hybrid energy system comes with various technical challenges, particularly in determining the optimal sizing and source combination that ensures the highest level of reliability, cost-effectiveness, and sustainability. In this context, achieving the optimal size configuration is a key factor in enhancing reliability while minimizing expenses. Consequently, there is a growing interest in creating intelligent technologies and algorithms to optimize the size of these systems[16][17][18]. Additionally, numerous studies focusing on the sizing and optimization of hybrid systems are being conducted, with the utilization of HOMER software[19][20].

So far, extensive research has been carried out on modeling, sizing, and optimizing techniques for hybrid renewable energy systems in various regions of Morocco[21]. For instance, L. Bousselamti, W. Ahouar, and M. Cherkaoui conducted a comprehensive study in Midelt city[22], focusing on optimizing the PV-CSP hybrid system. The study includes two models that simulate the hourly production of PV and CSP technologies over a year, and their results are rigorously validated using SAM software. In additional research, the authors investigate the impact of various parameters on the cost and energy production of PV, CSP, as well as PV-CSP hybrid system[23]. M. Chennaif, H. Zahboune, M. Elhafyani, and S. Zouggar [24] conducted a thorough examination of the optimal sizing for several hybrid systems based on the combination of PV, CSP and Wind turbines, with storage and without storage. They also offer detailed models for CSP, PV, and wind systems. Indeed, evaluating the production and performance of renewable energy systems, including hybrid systems, often involves the use of advanced modeling techniques.

These models are developed for the purpose of simulating, predicting, and analyzing the behavior of renewable energy systems under various conditions, including different climatic and design factors.

In this context, as an introduction to our forthcoming research on optimizing hybrid systems, the main objective of this work is to present the selected model derived from the literature, which is employed for estimating the hourly production of PV, CSP, and wind systems. Subsequently, the study allows for the simulation of capacity factors and annual power generation for these systems. The study focused on three different locations in Morocco: Midelt, Dakhla and Laayoune. This investigation is based jointly on the geographical coordinates of the three sites and the Meteorological data which was collected from a TMY file of a typical meteorological year data downloaded directly from the System Advisor Model (SAM) Software. To ensure the validity and accuracy of the obtained results, a comparison will be made with the estimates provided by the SAM, which is a widely recognized software tool used in the field for estimating energy production and performance of renewable energy systems.

2. Modelling Methodology:

Based on the research from the literature, it has been observed that simulation tools like SAM and MATLAB, along with other relevant software, are frequently used to evaluate the effectiveness of wind turbines, CSP, and PV plants[25]. Furthermore, numerous models are presented to simulate the behavior of these renewable energy systems under various operating conditions. This enables the investigation of their performance characteristics and facilitates a comprehensive study of their functionality, providing essential insights into their efficiency, reliability, and potential for optimization.

This paper presents the modeling of the PV, CSP and wind turbine systems using mathematical equations sourced from existing literature. The accuracy of these models is validated through SAM software.

Additionally, this work conducts simulations to assess the annual energy production and corresponding capacity factors of these systems over a one-year study period in three distinct locations in Morocco. This is by implementing the models in MATLAB, and the calculations of the hourly generated energy for each system and at each site can be conducted.

The paper presents a notable advancement in understanding the performance of these systems in diverse conditions and locations in Morocco. It also, offers a comparison of production between these renewable energy systems and locations, aiming to identify the system with the highest annual energy production and corresponding capacity factor.

Furthermore, the models presented in this study can contribute to improved system design by optimizing configurations and identifying the most efficient operating conditions.

The precise estimation of solar radiation received by the solar field holds significant importance as it serves as a fundamental factor in determining the electricity energy production potential of PV plants. This calculation takes into account factors such as temperature and the efficiency of the PV panels. Similarly, the electrical energy generated by CSP plants can be determined by considering both the overall efficiency and the solar radiation received by the solar field.

In contrast, the energy production of wind turbines relies on variables like wind speed and turbine efficiency. This study presents the solar radiation model and provides detailed calculations for determining solar position. The model and calculations are essential for accurately assessing solar radiation and understanding the position of the sun in relation to the solar field.

Three different locations in Morocco are considered: Laayoune, Dakhla, and Midelt. The geographical characteristics are presented in Table 1.

The schematic diagram of the models is presented in Fig. 2. The models take into account several inputs, including the geographical coordinates, solar position, and meteorological data. Furthermore, these models incorporate the specific characteristics of each system.

Table 1. The geographical characteristics

Site	Latitude in degree	Longitude in degree
Midelt	32.90	-4.70
Dakhla	23.41	-15.57
Laayoune	27,02	-13,38

The assessment of these systems involves comparing their annual electrical energy output and the corresponding capacity factor and examining the accuracy of models that illustrate the disparities between the calculations and results obtained from SAM.

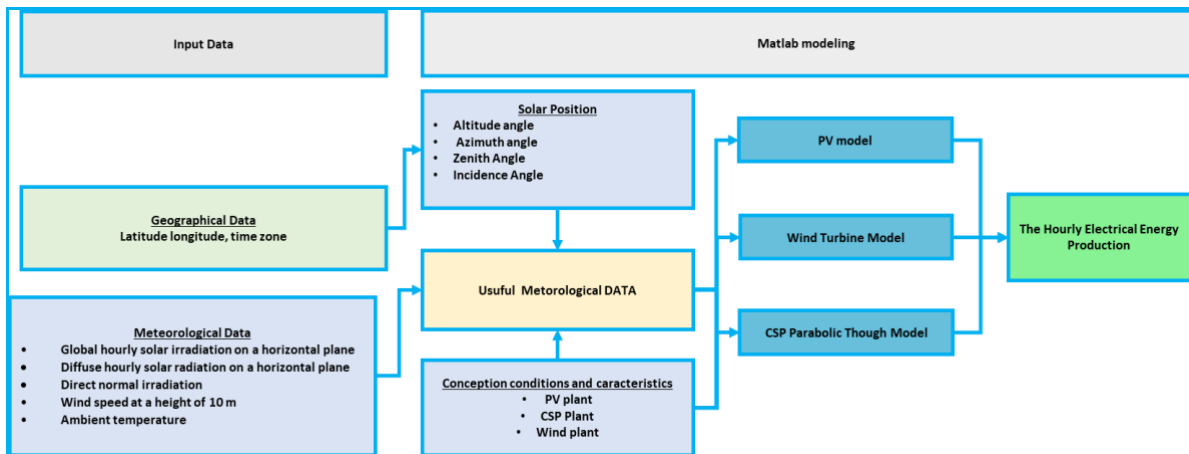


Fig 2. Representation of the Methodology's Schematic Diagram

Accurately modeling solar radiation over the study period is a fundamental step in designing and evaluating the performance of a solar energy system. Furthermore, the geographic location of the solar plant is a key factor in determining the availability and intensity of solar radiation, which directly impacts the system's performance and energy production potential. To accurately model solar radiation, it is crucial to consider factors such as solar angles and accurate calculations of solar radiation. Furthermore, it is essential to define the parameters of the solar field based on the specific type of solar technology employed. For instance, in the case of a CSP plant, the modeling would involve simulating a field consisting of parabolic troughs, while for a PV plant, the focus would be on modeling the photovoltaic modules.

3. Model Description

In this section, we present a concise depiction of the examined system, as visualized in Fig.2. The study delves into three specific renewable energy systems: PV, CSP, and Wind systems.

3.1. Solar Position

The solar position is extremely important in determining the amount of solar radiation that a solar energy system will receive. The sun's position changes every hour during the day and every day during the year, so it is necessary to model the solar coordinate systems throughout the year to predict the amount of solar radiation that the system will receive. By considering these changes, we can provide precise estimations for solar energy generation.

Geographical data of the chosen locations are utilized as input for the model to simulate and forecast the performance of a solar energy system. This data typically consists of the latitude, φ , longitude, λ , and the orientation angle of the solar energy system. In this case, a south orientation is represented by an angle of zero radians. Solar declination, δ , Equation time, ET, Local standard time, LST, and the solar hour angle, h_a , was calculated through the equations provided by [26]. Then, those parameters are used to calculate the solar altitude angle, α_s , according to [27].

$$\alpha_s = \sin^{-1}(\sin(\delta) \cdot \sin(\varphi) + \cos(\delta) \cdot \cos(\varphi) \cdot \cos(h_a)) \quad (1)$$

φ is the latitude of the selected site.

In the case of fixed-tilt surfaces of PV module at a tilt angle β , the angle between the module surface's normal and the center of the Sun, which represents the solar incidence angle, θ_{PV} , can be calculated using the equation (2) according to [22]. The more the PV module surface's normal is aligned as much as possible to the solar beams, more the received irradiance flux is higher.

$$\theta_{PV} = \cos^{-1}[\sin(\alpha_s) \cos(\beta) - \cos(\alpha_s) \sin(\beta) \cos(\gamma - \gamma_s)] \quad (2)$$

Where, γ_s is the azimuth of the surface, it is equal to zero when the panels are oriented south, The calculation of the Solar azimuth angle, γ , is based on a reference [28].

As mentioned before, the previous expression of incidence angle can be used only for fixed-tilt surfaces. This is the case of PV solar parks with no tracking system. In the case of a CSP thought collector, characterized by an azimuth tracking which refers to the technique of fixing the surface tilt angle while continuously adjusting the surface azimuth angle to align with the sun's azimuth angle. this method maximizes the collection of solar energy and is commonly employed in large-scale solar power plants where optimal energy production is essential [26]. Thus, the calculation for determining the angle of incidence on the collector is as follows[29]:

$$\theta_{CSP} = \cos^{-1}(\sqrt{\cos^2(\theta_z) + \cos^2(\delta) \sin^2(h_a)}) \quad (3)$$

With θ_z is the Zenith angle, in this case, it's calculated also according to[29].

The efficiency of a solar system is directly impacted by solar radiation[22]. To accurately estimate the energy potential of solar systems, it is crucial to assess the meteorological data available, specifically solar irradiation for solar energy systems. However, the available data is sometimes not exactly what we need as input to the predicting model of these systems. Typically, Global Horizontal Irradiance is the most common component of solar irradiance to be measured, it's usually measured on horizontal planes, whereas solar collectors are not installed horizontally but at a certain angle or with a tracking system to optimize solar radiation interception. Consequently, it is necessary to convert the available meteorological data into useful meteorological data that can be used as input for modeling.

After the solar position was defined (Solar altitude and azimuth angles), taking into consideration the available data, the initial step is to estimate the hourly global solar radiation received by solar collectors, G_t , which is composed of three main components: beam, G_b , diffuse, G_d , and reflected, G_r , and calculated using Equation (4):

$$G_t = G_b + G_d + G_r \quad (4)$$

To do so, several models are proposed. In the majority of these models, mathematical expressions are employed to estimate both direct and reflected radiation. However, there is variability among the models in terms of estimating diffuse

radiation. In our proposed models, we utilize the HDKR model [30] to calculate diffuse radiation, which is also utilized in the SAM software[26].

3.2. PV Plant Model Equations

The chosen PV model focuses on large utility-scale PV farms. Several important factors and considerations are taken into account in the model to determine the proper sizing of PV components. These factors include the maximum number of solar panels that can be connected in a series, referred to as a "string," the maximum number of strings that can be connected to a single inverter, and the total number of inverters needed. By considering these factors, the model ensures that the PV arrays are sized optimally to meet the desired system capacity.

For PV systems, multi-crystalline technology is commonly used because it holds a significant market share [31]. Unlike CSP systems, Photovoltaic (PV) surfaces are positioned in a fixed orientation, tilted upwards towards the South horizon. The angle of tilt is equivalent to the local latitude, without any horizontal tracking. This orientation is often selected to optimize the annual energy production, especially in countries such as Morocco. The most relevant parameters for the photovoltaic Plant are provided from the SAM library.

The temperature at which PV panels operate, T_c , is calculated based on their rated operating temperature, as defined in Equation 7 [32].

$$T_c = T_{amb} \left(\frac{G_t}{G_{noct,ref}} \right) (T_{noct} - T_{noct,ref}) \left(1 - \frac{\eta_{ref}}{\tau\alpha} \right) \left(\frac{U_{noct}}{5.7 + 3.8V_{wind}} \right) \quad (5)$$

The ambient temperature is denoted by T_{amb} , a nominal operating cell temperature, $T_{noct,ref}$, of 20°C and solar radiation, $G_{noct,ref}$, of 800W/m². The heat transfer factor is represented by U_{noct} , while V_{wind} is the wind speed.

To determine the actual efficiency of the PV panel, η_{pv} , Equation (6) can be used, which involves determining the transfer absorption factor ($\tau\alpha$)[32]:

$$\eta_{pv} = \eta_{ref} \left(1 + \gamma_t (T_c - T_{ref}) \right) \quad (6)$$

Where η_{ref} represents the nominal efficiency of the PV module, while γ_t is the temperature factor (experimentally measured by the constructor). Additionally, T_{ref} , is the temperature of the PV module under standard test conditions.

Equation (7) allows for the calculation of the Peak power output of the PV plant. Where N_{module} represents the total number of PV Modules; A_{module} represents the active area of each individual PV module, and $\eta_{pv,i}$ represents the efficiency of the panels.

$$P_{DC,peak,i} = \eta_{pv,i} G_i A_{module} N_{module} \quad (7)$$

Equation (8), which takes into account the efficiency of the inverter, $\eta_{inverter}$, can be used to estimate the power output of the PV system. Finally, a derating factor, f_{losses} , is used to account for secondary losses, including factors like dirt, wire loss, and panel shadows

$$P_t = P_{DC,peak,i} \eta_{inverter} f_{losses} \quad (8)$$

3.3. Wind Turbine Modeling:

Currently, Wind turbines with variable speeds are currently the most widely installed type[33]. In wind energy studies, these turbines are typically approximated using common equations to model the manufacturer's power curve. The power curve can be divided into four operational regions as depicted in Fig. 3 and described as follows: Region A represents wind speeds below the cut-in speed, at which point the wind turbine remains inactive and does not generate power; Region B includes wind speeds above the cut-in speed, allowing the turbine to generate power and adhere to Betts' Law, with a theoretical maximum utilization factor of 0.593 [32]; Region C represents the nominal wind speed range in which the turbine operates at peak efficiency and produces maximum power and Region D which includes wind speeds greater than the cut-out speed.

Wind turbines typically provide valuable information for power generation in regions A, C, and D. However, understanding the power curve in region B still presents challenges and remains complex [36]. In literature, several expressions to do this approximation can be found[37]. C. Carrillo, A. F. Obando Montaña, J. Cidrás, and E. Díaz-Dorado [33] and V. Sohoni, S. C. Gupta, and R. K. Nema [38] performed a comprehensive examination that evaluated the frequently employed equations used to represent the power curves of variable-speed wind turbine generators. Additionally, a parametric model for wind turbine power curves had been presented[36].

Within Region B, where wind speeds fall between the cut-in and the rated wind speeds, the wind power production can be determined using Equation (9), which This equation takes into account variables such wind speed, V_{ws} , air density, ρ , rotor area, A_r , and power coefficient C_p .

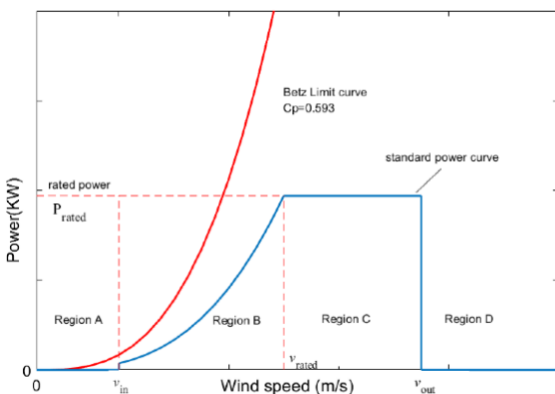


Fig. 3. Power Curve[35]

As a result, the expression for the output power is formulated as follows[39]:

$$P_w = \begin{cases} 0 & \text{if } V_{ws} < V_{in} \text{ or } V_{ws} > V_{out} \\ \frac{1}{2} \rho \cdot A_r \cdot C_p \cdot V_{ws}^3 & \text{if } V_{in} \leq V_{ws} < V_{rated} \\ P_{rated} & \text{if } V_{ws} \geq V_{rated} \end{cases} \quad (9)$$

where P_{rated} is the rated electrical power; V_{in} is the cut-in wind speed; V_{rated} is the rated wind speed; and V_{out} is the cut-off wind speed.

Wind speed is usually measured at 10 m [40], To compute the power output for a specific height and wind speed, the initial step involves determining the wind speed at the turbine hub height. That using the Equation (10), which allows us to calculate the wind speed at the desired height from the wind speed at a specific hub height h_0 and α .

$$V_{ws,h} = V_{ws,0} \left(\frac{h}{h_0} \right)^\alpha \quad (10)$$

$V_{ws,h}$ and $V_{ws,0}$ are the wind speed at the hub height h and h_0 respectively. The Hub Height is provided from the Turbine input page[41], α is the wind shear which is a dimensionless constant used to describe the wind speed profile in the atmosphere, is approximately 1/7, or more precisely 0.14 when there is no specific site data[39]. It is crucial to bring attention that wind direction could change as a function of height[36]. for our study, the effect of wind direction on wind production is not considered.

3.4. CSP Model:

The solar power plant simulation is developed using MATLAB. The CSP plant model incorporates a molten salt central-receiver system that is connected to a two-tank molten salt direct thermal energy storage, which is then coupled to a Rankine cycle[42].

As parabolic trough solar concentrators accept only DNI, and on the basis of [43],The total absorbed energy from the solar Field, $P_{CSP,absorbed}$, can be calculated as a function of the solar field area, A_{sf} , The overall efficiency, η_{SF} , as follow:

$$P_{CSP,absorbed} = \eta_{SF} \cdot A_{sf} \cdot DNI \quad (11)$$

The overall efficiency η_{SF} is given by the product of the cos-loss efficiency, $\cos(\theta_{csp})$, the geometry effect efficiency, η_{geo} , the incidence angle Modifier-loss efficiency, η_{IAM} , the shadow-loss efficiency, η_{shadow} , the end-loss efficiency, $\eta_{endlosses}$, the mirror reflectance, ρ_m , the tracking error, η_{track} , the general error, η_{gen} , and the mean cleanliness factor, Cl.

$$\eta_{SF} = \cos(\theta_{csp}) \cdot \eta_{geo} \cdot \eta_{IAM} \cdot \eta_{shadow} \cdot \eta_{endlosses} \cdot \rho_m \cdot \eta_{track} \cdot \eta_{gen} \cdot Cl \quad (12)$$

In the case of CSP parabolic troughs, the angle of incidence of solar radiation on a north-south axis tracking can be calculated using equation (3)[43].

The empirical fit for the incidence angle modifier is based on experimental data specific to a particular type of collector [44]. An expression for the incidence angle modifier used in the solar field component model is given in the Technical Manual for the SAM Physical Trough Model [45]. The shadow-loss efficiency could be calculated using the reference[45], The range of values for total shadow-loss efficiency is between 0.5 and 1.0. If the shadowing efficiency is less than 0.5, the solar field is unlikely to operate successfully[45]. End-loss occurs naturally when the reflected sunlight doesn't reach the absorber tube. This effect can be reduced by installing a long row. The expression for the end losses is given by [42][43]. The parameters of η_{geo} , ρ_m and η_{track} can be measured according to reference [43]. The present study utilizes the parameters obtained from the SAM library.

The total efficiency, η_{SF} , is determined through the combination of the previously computed factors along with tracking error, mirror reflectance, geometry effects, and general error inputs.

The thermal energy output of the solar field, $P_{CSP,thermal}$, is computed by subtracting the thermal losses, P_{Losses} , from the total absorbed power, P_{incid} .

$$P_{CSP,thermal} = P_{incid} - P_{Losses} \quad (13)$$

Another expression, using the solar field thermal efficiency, $\eta_{SF,therm}$, and the Storage efficiency, $\eta_{storage}$, is also presented:

$$P_{CSP,thermal} = \eta_{SF,therm} \cdot P_{incid} \cdot \eta_{storage} \quad (14)$$

The calculation of thermal losses in a CSP receiver can be a complex process due to various factors that can impact the efficiency of the system, including convection, conduction, and radiation losses[46]. Through the application of metal glass evacuated tubes and specialized surface coatings on the receiver, efforts have been made to minimize convection and radiation losses[47]. A review is provided on different theoretical and experimental research conducted to enhance the thermal and optical efficiency of solar thermal systems[47]jsmart, Several models are presented to predict the efficiency of a parabolic trough collector[42], an extensive discussion on various techniques aimed at improving the optical and thermal efficiency of the parabolic trough collector plant[48]. The net electrical power output of CSP can be determined using Equation (15)[21]:

$$P_{CSP,elec} = \eta_{PB} \cdot P_{CSP,thermal} \quad (15)$$

Where $P_{thermal}$ is the total available thermal energy for the power block and η_{PB} is the overall power block efficiency which can be calculated as follows:

$$\eta_{PB} = \eta_{turb} \cdot \eta_{generator} \cdot (1 - \xi) \quad (16)$$

The quantity, ξ , represents the parasitic loss, which usually ranges from 4% to 13% of the nominal gross power output of the plant. The parasitic consumption considers internal electricity usage for plant operation, such as running heat transfer fluid pumps, tracking systems and others[49], or electrical losses on the generator and on the transformer[21].

$\eta_{generator}$ is the nominal generator efficiency, η_{turb} is the constant thermodynamic efficiency of an ideal Rankine cycle, A value of 10% is suggested for ξ [49], $\eta_{generator}$ is set to 97% and η_{turb} it's equal to 37,6% according to [21]. Typically, the overall efficiency of the thermal power block of the plant is assumed to be 40%[49].

4. Meteorological Data

The chosen sites exhibit similar weather characteristics with regards to Direct Normal Irradiance (DNI) as presented in Fig. 4 Dakhla is known for its high solar radiation, with the maximum DNI occurring in April and reaching up to 366 W/m². Laayoune, on the other hand, has a maximum DNI of approximately 332 W/m² in June. Midelt experiences its highest DNI in July, with values reaching up to 305 W/m².

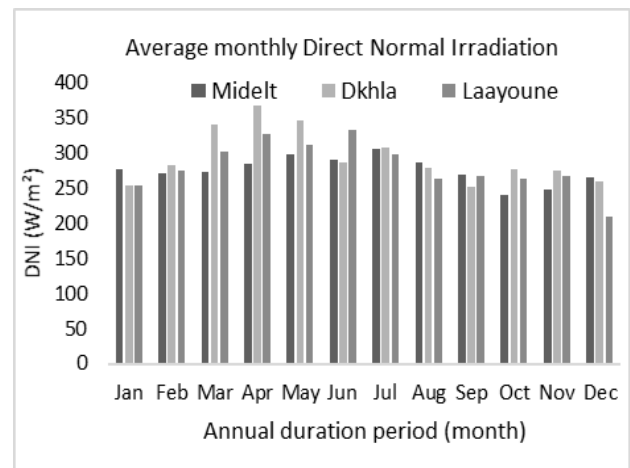


Fig. 4. DNI under the annual duration period.

As mentioned before, Sometimes the available data is not exactly what we need as input to our behaviour models, for example: global solar irradiance is measured on horizontal planes, whereas solar collectors are not installed horizontally but at a certain angle or with a tracking system to optimize solar radiation interception. It is, therefore, necessary to convert the available meteorological data into "useful meteorological data for our models. Using the calculations described previously, the average global radiance received on a PV tilt module and the parabolic trough collector are calculated. The results of the calculated average Global Irradiance received on the tilt PV module are presented in Fig. 5.

The daily variations of mean wind speeds at a height of 10 m for the sites considered are presented in Fig. 6, it can be seen, that the maximum daily average wind speed for Laayoune is 7,94 m/s, whereas for Midelt, it is 3,61 m/s and 7,42 m/s in Dakhla. Additionally, the mean daily average wind speed for Dakhla is 6.02 m/s and 6.22 m/s for

Laayoune, which are notably higher than the mean daily average wind speed for Midelt, which is 2.32 m/s.

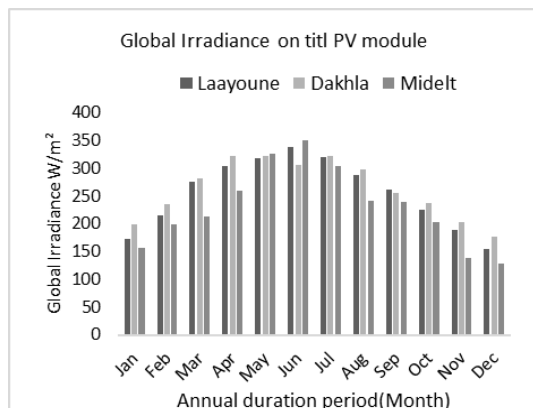


Fig. 5. Global Irradiance received on tilt PV module.

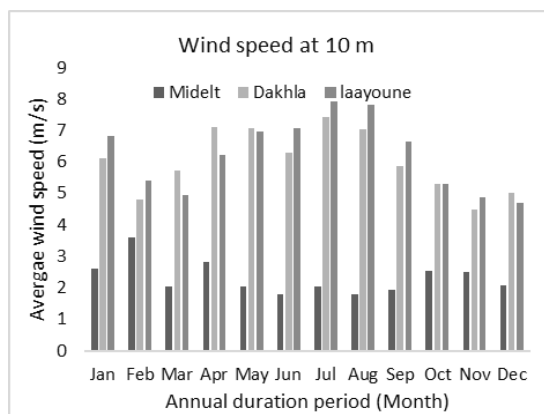


Fig. 6. Wind speed at a height of 10 m.

Table 2. The Annual electrical energy production calculated by SAM and the adopted model

Power PV plant MW	Annual electrical energy production (GWh)								
	Midelt			Dakhla			Laayoune		
	SAM	Model	difference %	SAM	Model	Difference %	SAM	Model	difference %
10	19,13	18,64	2,55%	20,32	19,76	2,56%	20,78	20,16	2,96%
20	38,5	37,25	3,25%	40,95	39,51	3,30%	41,88	40,30	3,78%
30	57,66	55,89	3,06%	61,3	59,27	3,26%	62,68	60,45	3,56%
40	77,01	74,50	3,25%	81,91	79,03	2,33%	83,76	80,59	3,78%
50	96,16	93,13	3,15%	102,26	98,78	3,40%	104,57	100,74	3,66%
60	115,51	111,74	3,26%	122,87	118,54	3,52%	125,64	120,88	3,79%
70	134,67	130,39	3,18%	143,22	138,30	3,44%	146,45	141,04	3,70%
80	153,82	149,06	3,09%	163,57	158,10	3,34%	167,26	161,24	3,60%
90	173,17	167,71	3,16%	184,18	177,90	2,92%	188,33	181,42	3,67%
100	192,33	186,29	3,14%	204,53	197,59	3,39%	209,14	201,51	3,65%

The slight difference observed between the proposed model and the SAM simulation can be attributed to simplifications in the models and the omission of certain factors. In the PV-selected model, the calculation of panel and inverter efficiencies is simplified, and factors such as shading losses and nightly inverter energy consumption are not considered. On the other hand, the SAM model takes into

5. Results and Discussions

In the analysis of energy production, two important factors are considered: capacity factor and annual electrical energy production, the results of the annual electrical energy production in gigawatt-hours (GWh) for PV plants with capacities ranging from 10 MW to 100 MW are presented in Table 2.

The energy production is evaluated for the three locations. The results include energy production values obtained from the SAM simulation, as well as the percentage differences between the SAM model and the selected model.

For a 10 MW PV plant, Laayoune has the highest annual energy production (20.78 GWh), followed by Midelt (19.13 GWh), and Dakhla (18.64 GWh). As the capacity increases to 100 MW, the trend remains consistent, with Laayoune having the highest annual energy production (201.51 GWh), followed by Midelt (192.33 GWh), and Dakhla (186.29 GWh). Laayoune generally exhibits the highest energy production, followed by Midelt and Dakhla, highlighting the influence of site-specific factors on energy output. The comparison between the results obtained from the proposed model and the SAM simulation reveals a small difference in the estimated energy production values. The percentage differences range from 2.55% to 3.78%, with the proposed model generally predicting slightly higher energy production compared to the SAM simulation.

account the sun's position for each time step in the weather file, utilizing a complex algorithm [26][50].

The results obtained from the calculation of the annual capacity factors for the PV plants in Midelt, Dakhla, and Laayoune are presented in Table 3. The results show that the PV plants in the three sites have capacity factors ranging from 22% to 24%. Laayoune stands out as the most favorable

location with the highest capacity factor, indicating its potential for efficient PV energy generation. The capacity factors obtained from both the SAM simulation and the selected PV model are in close agreement, indicating that the selected model is providing reliable estimates compared to SAM simulation results.

Table 3. The average capacity factor of the PV system

Site		Midelt	Dakhla	Laayoune
Capacity Factor	SAM	22,56%	23,20%	23,90%
	selected Model	22,00%	23,00%	23,80%

Three wind generators are included in the analysis for wind energy systems, and their technical specifications can be found in Table 4. These specifications were sourced from the wind power database [51]. Additionally, the turbines have nominal powers of 750 kW, 900 kW, and 1000 kW. The power curves shown in Figure 7 were also obtained from the same reference.

Fig. 7. Power curves of the wind turbines.

Based on the reference [36], typical values for the power coefficient and air mass density are commonly used in our calculations to simplify the process and improve the accuracy of the proposed model.

Table 4. Technical Specifications for Wind Turbines

Wind Turbine	V_{in}	V_{rated}	V_{out}	P_{rated}	A_r
	m/s	m/s	m/s	MW	m
Mitsubishi MWT62-1000	5	13.5	25	1.0	61.4
EWT DW54-900	2.5	13	25	0.9	54
Unison U50	2.5	12.5	25	0.75	50

The hourly electrical production of the selected wind turbines was calculated in the Laayoune site using 8760 hourly wind speed values derived from a TMY file, spanning over the course of a typical year. The results obtained from the calculations are presented in the form of a power curve for each wind turbine. Subsequently, a comparison was made between the obtained power curves and the power curves generated by the SAM model.

The power curves that were obtained can be seen in Fig. 8, Fig. 9 and Fig. 10 for Unison U50-750, EWT 54-900 and MWT 64-1000 respectively. It clearly appears that the selected wind turbine Model and the SAM wind turbine Model, generated similar power curves, with some slight differences in their prediction of the turbine's power output. In fact, a little difference was found and it's observed in the region B. Consequently, as the observed difference between the two models is small, the wind turbine model proposed in this study appears to be effective in predicting wind power production.

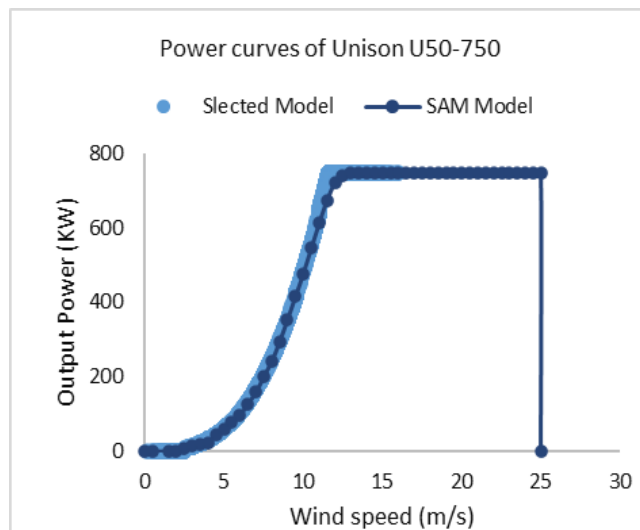


Fig. 8. Power curves of Unison U50-750

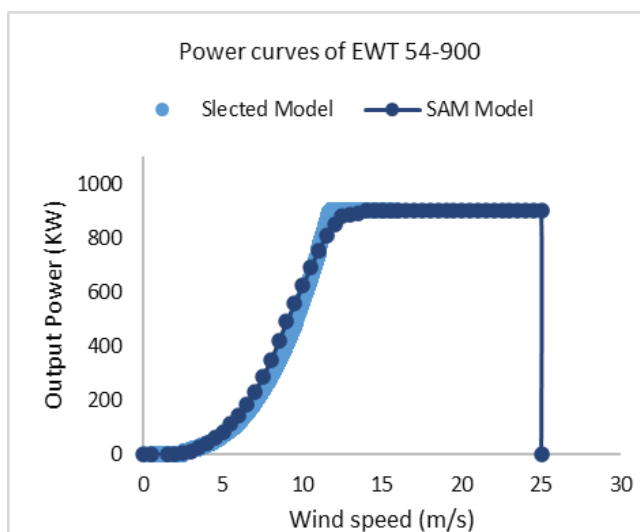


Fig. 9. Power curves of EWT 54-900

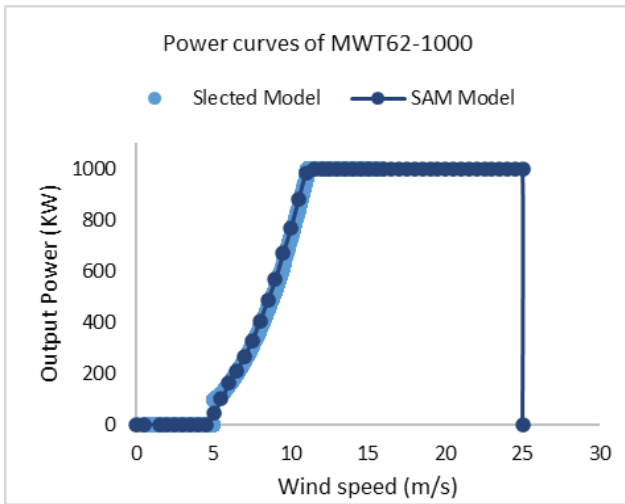


Fig. 10. Power curves of MWT 62-100

Table 5. Annual energy production and corresponding capacity factor of the wind turbines

Turbines	Midelt		Dakhla		Laayoune	
	C_f	E_{annual} (GWh)	C_f	E_{annual} (GWh)	C_f	E_{annual} (GWh)
Mitsubishi MWT62-1000	3,8 %	0,33	42,9 %	3,76	46,6 %	4,08
EWT 54-900	4,1 %	0,32	32,6 %	2,57	45,7 %	3,6
Unison U50	4,3 %	0,28	31,4 %	2,06	42,9 %	2,82

The values obtained from this study can be compared with those of Y. El Khchine and M. Sriti, [52], who conducted a similar analysis on the annual capacity factor of wind turbines in Dakhla and Laayoune. In their study, they determined that the capacity factor reached a peak of 41.3% in both Laayoune and Dakhla.

To ensure a profitable investment in wind energy, it is recommended to choose wind turbines with a capacity factor of at least 25%. This recommendation is widely supported by various sources in the field, including references [53] and [54]. Based on this recommendation, our analysis shows that three wind turbines are suitable for grid integration at Laayoune and Dakhla, as their capacity factors exceed 25%. This makes them economically viable for wind energy production. However, this is not the case in Midelt, where the capacity factor is less than 5%, indicating that wind energy investment may not be profitable in that location.

Laayoune presents the highest annual energy generation among the three wind turbines, ranging from 2.82 GWh to 4.08 GWh. This indicates the most productive wind resource at this location. While, the lowest annual energy generation is presented in Midelt and ranges from 0.28 GWh to 0.33 GWh.

Based on these comparisons, it can be concluded that both Dakhla and Laayoune offer better wind turbine performance compared to Midelt. However, Laayoune stands out as the most favorable location with the highest capacity factors and annual energy generation.

Comparing the results between the three sites, we can see that the capacity factor and annual energy production

The utilization of the Selected model enables us to accurately calculate the hourly electrical energy generation. Furthermore, by employing this model, we are able to determine the annual electrical energy generated, as well as calculate the corresponding capacity factor. Table 5 presents the calculated capacity factor and annual energy generated by each wind turbine.

Across all three sites, the Mitsubishi MT62-1000 wind turbine consistently outperforms the other turbines in terms of capacity factor, as shown in Table 5. It achieves the highest capacity factors and generates the most annual electrical energy. Additionally, the table reveals that the Laayoune site exhibits the highest Capacity Factor, ranging from 42.9% to 46.6%, indicating a significant potential for wind energy. Conversely, the Midelt site has the lowest potential with a capacity factor of less than 5%.

values vary considerably between locations for the selected turbines. Laayoune has the highest capacity factor and annual energy production for all wind turbines, while Midelt has the lowest values. This indicates that the performance of a wind turbine can be greatly influenced by its suitability for a specific location.

When considering the calculation methods for CSP plants with TES storage, hypotheses play a crucial role in simplifying the complex heat transfer and mass transfer calculations involved in the system. In our study, several hypotheses are taken into account.

Firstly, it is assumed that there are no significant heat losses during the transfer of thermal energy from the solar collector system to the TES system. This assumption allows us to simplify the calculations by disregarding any energy losses that may occur during the heat transfer process.

Secondly, it is assumed that all the thermal energy generated by the solar collector system is effectively and entirely transferred to the TES system without any losses. This assumption simplifies the calculation process by assuming that the TES system receives the full amount of thermal energy produced by the CSP plant.

Thirdly, it is assumed that the losses occurring in the TES system are minimal and can be neglected. This assumption implies that the TES system is highly efficient in storing and retaining thermal energy without significant losses, allowing us to simplify the calculations by considering minimal energy losses within the storage system.

Lastly, it is assumed that both the heat transfer fluid and the TES system operate under conditions where their

respective energy levels remain above the freezing point or solidification temperature. This assumption ensures that the heat transfer fluid does not freeze or solidify, and that the TES system maintains its functionality and energy storage capabilities.

By assuming negligible heat losses, complete thermal energy transfer, limited storage losses, and energy equilibrium within the heat transfer fluid and TES system, the calculations become more manageable. Moreover, these assumptions simplify the complex heat transfer and mass transfer calculations, enabling a more simplified analysis of the system's performance.

For the study of the CSP system, we present an analysis of the capacity Factor and the annual electrical energy generation of a CSP plant of 50 MW. The solar collectors of the plant utilize single-axis tracking of the sun to optimize the concentration of reflected solar radiation towards the absorber tube throughout the day.

The efficiency of the solar field is calculated using the equations presented previously. For this study, the Euro trough ET 150 solar collector and Schott PTR80 receiver were utilized, with Therminol VP-1 as the heat transfer fluid. The design characteristics of the solar field, obtained from the SAM (System Advisor Model) library, include a design irradiation of 950 W/m², a design ambient temperature of 25 °C, a design wind velocity of 5 m/s, a row spacing of 15 m, a design inlet temperature of 290 °C, and a design outlet temperature of 390 °C. The power block model employed was the Rankine Cycle, with a cycle efficiency of 40% and a generator efficiency of 96%. The thermal storage system utilized Hitec solar salt as the thermal storage fluid, demonstrating an efficiency of 98.5%. The thermal energy storage (TES) system followed a two-tank direct configuration.

The obtained results of the electrical energy production of a 50 MW CSP plant, calculated using the chosen model and simulated by SAM, are presented in Table 6. Additionally, Table 7 provides the calculated average annual Capacity factor. The results indicate that the location plays a crucial role in determining the plant's performance, as the values vary based on specific conditions at each location. Dakhla has the highest annual electrical energy output of 177,47 GWh, with a capacity factor of 40.5%. This means that the Dakhla location is the most suitable for operating a CSP plant as it has been consistently generating electricity throughout the year. On the other hand, Midelt has the lowest annual electrical energy output of 150,71 GWh with a capacity factor of 34.4%. Laayoune's annual electrical energy output of 165,12 GWh and a capacity factor of 38% fall between the other two locations.

The proposed model makes simplifying assumptions regarding heat losses, thermal energy transfer, storage losses, and energy equilibrium in the CSP plant. These assumptions are intended to simplify calculations and analyze the plant's performance in a more manageable way. However, because of these simplifications, the calculated values tend to be higher than those simulated by SAM, which takes into account a wider range of factors and provides a more comprehensive and accurate representation of the plant's performance.

To compare the productivity of solar and wind systems in these locations, we can analyze the calculated values of electrical energy generation for each technology. By examining the energy generation data, we can assess the relative performance and efficiency of solar and wind systems in these locations. This analysis will provide valuable insights into the productivity of each technology, helping inform decisions regarding their suitability and potential for deployment in these areas.

Table 6. The Annual electrical energy production calculated by SAM and the adopted model

Power plant MW	Annual electrical energy production (GWh)								
	Midelt			Dakhla			Laayoune		
	SAM	Model	difference %	SAM	model	Difference %	SAM	Model	difference %
50	150.71	158.24	4.99	177.47	185.94	4.77	165.12	173.37	4.98

Table 7. The average annual Capacity factor

Site	Midelt	Dakhla	Laayoune
Capacity Factor	34.4%	40.5%	38%
Proposed Model	36.1%	42.4%	39.5%

To conduct this comprehensive comparison, a simulation was carried out for a 50 MW power plant using PV, CSP, and wind technologies. By conducting this simulation for all three technologies, it was possible to evaluate and compare their productivity and performance in terms of electrical energy generation. Additionally, the simulation enabled the computation of the average annual capacity factor, offering valuable insights into the utilization and efficiency of each system.

Figure 11 displays the comparative outcomes of the annual energy generation for 50 MW PV, CSP, and wind facilities across the three designated locations

It appears that, wind power outperforms both PV and CSP, in Laayoune and Dakhla. indicating that wind energy is the most efficient technology for electricity generation in these locations, which is not the case of Midelt where the wind production is small in the order of 17 GWh.

Laayoune and Dakhla boast the highest energy generation among all technologies, making them ideal for renewable energy production. These regions possess an abundance of wind resources and great solar potential, creating highly favorable conditions for generating clean energy.

Fig. 11. The annual energy generation of a 50 MW plant

6. Conclusions

This paper focuses on presenting models for PV, CSP, and wind turbine systems, utilizing mathematical equations sourced from existing literature. The accuracy of these models is validated through SAM software. Additionally, the paper conducts simulations to assess the annual energy production and corresponding capacity factors of these systems over a one-year study period in three distinct locations in Morocco.

The paper presents a notable advancement in understanding the performance of these systems in diverse conditions and locations in Morocco. It also, offers a comparison of production between these renewable energy systems and locations, aiming to identify the system with the highest annual energy production and corresponding capacity factor.

In conclusion, the findings from this study demonstrate that Dakhla, Midelt, and Laayoune exhibit high solar potential, as evidenced by the capacity factors of the PV plants in these locations. The capacity factors, ranging from 22.56% to 23.90%, indicate the efficient utilization of solar resources and the substantial generation of electrical energy.

Comparing the capacity factors among the three locations, it is apparent that both Dakhla and Laayoune offer better wind turbine performance compared to Midelt. However, Laayoune stands out as the most favorable location, with the highest capacity factors and annual energy generation. Therefore, prioritizing coastal locations like Laayoune would likely yield better results in terms of electricity generation when considering wind turbine deployment. Furthermore, the relatively close values of generated energy among Dakhla, Laayoune, and Midelt

suggest that all three locations possess significant solar potential. Despite variations in annual electrical energy output and capacity factor, it can be concluded that CSP technology can generate a substantial quantity of energy in these areas.

The presented models for PV and CSP demonstrate a good level of accuracy, with a difference of approximately 3-5% compared to the SAM model. Similarly, the power curves obtained from the selected wind turbine model closely resemble the power curve, with only slight differences. The differences observed between the chosen models and the SAM models can be attributed to the simplifications made in the presented models. Nevertheless, these findings suggest that the models can be relied upon for estimating energy production in these areas.

In summary, the study results highlight the suitability of Laayoune and Dakhla for renewable energy production, with their abundant wind resources and high solar potential. By integrating both wind and solar energy systems at these sites, it becomes possible to generate renewable energy consistently, even during periods of limited solar radiation. These hybrid systems can contribute to stable energy production while reducing costs and lead to a more robust and reliable energy supply, reducing dependence on non-renewable sources. Additionally, the simplicity and reliability of the models used in this study make them suitable for estimating energy production in such hybrid systems. Moving forward, future research will focus on evaluating and optimizing hybrid systems that integrate solar and wind energy. This analysis aims to assess the feasibility, advantages, and potential optimizations of combining both energy sources, ultimately enhancing renewable energy generation in these locations.

References

- [1] L. Mellouk, M. Ghazi, A. Aaroud, M. Boulmalf, D. Benhaddou, and K. Zine-Dine, "Design and energy management optimization for hybrid renewable energy system- case study: Laayoune region," *Renewable Energy*, vol. 139, no. 2019, pp. 621–634, 2019, doi: 10.1016/j.renene.2019.02.066.
- [2] Z. Aqachmar, A. Allouhi, A. Jamil, B. Gagouch, and T. Kousksou, "Parabolic trough solar thermal power plant Noor I in Morocco," *Energy*, vol. 178, pp. 572–584, 2019, doi: 10.1016/j.energy.2019.04.160.
- [3] M. Makkiabadi, S. Hoseinzadeh, A. Taghavirashidizadeh, M. Soleimaninezhad, M. Kamyabi, H. Hajabdollahi, M. M. Nezhad and G. Piras "Performance evaluation of solar power plants: A review and a case study," *Processes*, vol. 9, no. 12, pp. 1–26, 2021, doi: 10.3390/pr9122253.
- [4] International Renewable Energy Agency (IRENA), "Renewable Energy Statistics 2022 About IRENA," 2022. [Online]. Available: <https://www.irena.org/> (Last accessed date: 23/01/2023)

- [5] M. Azeroual, A. El Makrini, H. El Moussaoui, and H. El Markhi, "Renewable energy potential and available capacity for wind and solar power in Morocco towards 2030," *Journal of Engineering Science and Technology Review*, vol. 11, no. 1, pp. 189–198, 2018, doi: 10.25103/jestr.111.23.
- [6] A. Mohamed and H. El Markhi, "Renewable Energy Potential and Available Capacity for Wind and Solar Power in Morocco Towards 2030," no. February, 2018, doi: 10.25103/jestr.111.23.
- [7] M. Boulakhbar, B. Lebrouhi, T. Kousksou, S. Smouh, A. Jamil, M. Maaroufi and M. Zazi., "Towards a large-scale integration of renewable energies in Morocco," *Journal of Energy Storage*, vol. 32, no. May, p. 101806, 2020, doi: 10.1016/j.est.2020.101806.
- [8] T. Haidi, B. Cheddadi, F. El Mariami, Z. El Idrissi, and A. Tarrak, "Wind energy development in Morocco: Evolution and impacts," *International Journal of Electrical and Computer Engineering*, vol. 11, no. 4, pp. 2811–2819, 2021, doi: 10.11591/ijece.v11i4.pp2811-2819.
- [9] H. Ait Lahoussine Ouali, A. Alami Merrouni, S. Chowdhury, K. Techato, S. Channumsin, and N. Ullah, "Optimization and Techno-Economic Appraisal of Parabolic Trough Solar Power Plant under Different Scenarios: A Case Study of Morocco," *Energies*, vol. 15, no. 22, 2022, doi: 10.3390/en15228485.
- [10] K. Attari, A. Elyaakoubi, and A. Asselman, "Performance analysis and investigation of a grid-connected photovoltaic installation in Morocco," *Energy Reports*, vol. 2, no. December 2015, pp. 261–266, 2016, doi: 10.1016/j.egyr.2016.10.004.
- [11] N. Mrabet, C. Benzazah, and A. El Akkary, "Technical Analysis and Comparative Study of three Wind Turbines for a 50MW wind farm in Laayoune City Morocco," *ITM Web of Conferences*, vol. 46, p. 01002, 2022, doi: 10.1051/itmconf/20224601002.
- [12] A. H. Fathima and K. Palanisamy, "Optimization in microgrids with hybrid energy systems - A review," *Renewable and Sustainable Energy Reviews*, vol. 45, pp. 431–446, 2015, doi: 10.1016/j.rser.2015.01.059.
- [13] M. Kharrich, O. H. Mohammed, and M. Akherraz, "Assessment of renewable energy sources in Morocco using economical feasibility technique," *International Journal of Renewable Energy Research*, vol. 9, no. 4, pp. 1856–1864, 2019, doi: 10.20508/ijrer.v9i4.10181.g7791.
- [14] G. GURSOY and M. Baysal, "Improved optimal sizing of hybrid PV/wind/battery energy systems," in 2014 International Conference on Renewable Energy Research and Application (ICRERA), Oct. 2014, pp. 713–716. doi: 10.1109/ICRERA.2014.7016478.
- [15] J. Zhang and H. Wei, "A review on configuration optimization of hybrid energy system based on renewable energy," *Frontiers in Energy Research*, vol. 10, no. August, pp. 1–15, 2022, doi: 10.3389/fenrg.2022.977925.
- [16] M. D. A. Al-falahi, S. D. G. Jayasinghe, and H. Enshaai, "A review on recent size optimization methodologies for standalone solar and wind hybrid renewable energy system," *Energy Conversion and Management*, vol. 143, pp. 252–274, 2017, doi: 10.1016/j.enconman.2017.04.019.
- [17] S. R.- Álvarez and J. Espinosa, "Multi-Objective Optimal Sizing Design of a Diesel- PV-Wind-Battery Hybrid Power System in Colombia," *International Journal of Smart grid*, vol. 2, no. 1, 2018, doi: 10.20508/ijsmartgrid.v2i1.12.g13.
- [18] K. D. Mercado, J. Jiménez, and M. C. G. Quintero, "Hybrid renewable energy system based on intelligent optimization techniques," in 2016 IEEE International Conference on Renewable Energy Research and Applications (ICRERA), Nov. 2016, pp. 661–666. doi: 10.1109/ICRERA.2016.7884417.
- [19] M. Longo, W. Yaïci, and F. Foadelli, "Hybrid Renewable Energy System with Storage for Electrification a Case Study of Remote Northern Community in Canada," *International Journal of Smart grid*, no. June, 2019, doi: 10.20508/ijsmartgrid.v3i2.58.g47.
- [20] I. M. Opedare, T. M. Adekoya, and A. E. Longe, "Optimal Sizing of Hybrid Renewable Energy System for off-Grid Electrification: A Case Study of University of Ibadan Abdusalam Abubakar Post Graduate Hall of Residence," *International Journal of Smart grid*, vol. 4, no. 4, 2020, doi: 10.20508/ijsmartgrid.v4i4.135.g110.
- [21] A. Bouramdane, "Scenarios of Large-Scale Solar Integration with Wind in Morocco : Impact of Storage , Cost , Spatio-Temporal Complementarity and Climate Change," 2021. [Online]. Available: <https://tel.archives-ouvertes.fr/tel-03518906>
- [22] L. Bousselamti, W. Ahouar, and M. Cherkaoui, "Multi-objective optimization of PV-CSP system in different dispatch strategies, case of study: Midelt city," *Journal of Renewable and Sustainable Energy*, vol. 13, no. 1, 2021, doi: 10.1063/5.0025928.
- [23] L. Bousselamti and M. Cherkaoui, "Modelling and Assessing the Performance of Hybrid PV-CSP Plants in Morocco: A Parametric Study," *International Journal of Photoenergy*, vol. 2019, 2019, doi: 10.1155/2019/5783927.
- [24] M. Chennaif, H. Zahboune, M. Elhafyani, and S. Zouggar, "Electric System Cascade Extended Analysis for optimal sizing of an autonomous hybrid CSP / PV / wind system with Battery Energy Storage System and thermal energy storage," *Energy*, vol. 227, p. 120444, 2021, doi: 10.1016/j.energy.2021.120444.
- [25] S. Sinha and S. S. Chandel, "Review of software tools for hybrid renewable energy systems," *Renewable and Sustainable Energy Reviews*, vol. 32, pp. 192–205, 2014, doi: 10.1016/j.rser.2014.01.035.

- [26] P. Gilman, A. Dobos, N. DiOrio, J. Freeman, S. Janzou and D. Ryberg, "SAM Photovoltaic Model Technical Reference Update SAM Photovoltaic Model Technical Reference Update," no. March, 2018.
- [27] S. Herrería-Alonso, A. Suárez-González, M. Rodríguez-Pérez, R. F. Rodríguez-Rubio, and C. López-García, "A solar altitude angle model for efficient solar energy predictions," *Sensors (Switzerland)*, vol. 20, no. 5, 2020, doi: 10.3390/s20051391.
- [28] M. E. Matius, M. Ismail 1, Y. Farm, A. E. Amaludin, M. A. Radzali, A. Fazlizan and W. K. Muzammil, "On the optimal tilt angle and orientation of an on-site solar photovoltaic energy generation system for sabah's rural electrification," *Sustainability (Switzerland)*, vol. 13, no. 10, 2021, doi: 10.3390/su13105730.
- [29] M. H. Mohamed, A. Z. El-Sayed, K. F. Megalla, and H. F. Elattar, "Modeling and performance study of a parabolic trough solar power plant using molten salt storage tank in Egypt: effects of plant site location," *Energy Systems*, vol. 10, no. 4, pp. 1043–1070, 2019, doi: 10.1007/s12667-018-0298-4.
- [30] M. Maleki Seyed Abbas; H. Hizam and Chandima Gomes, "Estimation of Hourly, Daily and Monthly Global Solar Radiation on Inclined Surfaces :Models Re-Visited," 2017, doi: 10.3390/en10010134.
- [31] M. Hosenuzzaman, N. A. Rahim, J. Selvaraj, and M. Hasanuzzaman, "Global prospects , progress , policies , and environmental impact of solar photovoltaic power generation," *Renewable and Sustainable Energy Reviews*, vol. 41, pp. 284–297, 2015, doi: 10.1016/j.rser.2014.08.046.
- [32] R. Zhai, H. Liu, Y. Chen, H. Wu, and Y. Yang, "The daily and annual technical-economic analysis of the thermal storage PV- CSP system in two dispatch strategies," *Energy Conversion and Management*, vol. 154, no. June, pp. 56–67, 2017, doi: 10.1016/j.enconman.2017.10.040.
- [33] C. Carrillo, A. F. Obando Montaña, J. Cidrás, and E. Díaz-Dorado, "Review of power curve modelling for windturbines," *Renewable and Sustainable Energy Reviews*, vol. 21. pp. 572–581, 2013. doi: 10.1016/j.rser.2013.01.012.
- [34] M. H. Ranjbar, H. Zanganeh, and K. Gharali, "Reaching the Betz Limit Experimentally and Numerically Reaching the betz limit experimentally and numerically," no. September, 2019, doi: 10.22059/EES.2019.36563.
- [35] Z. Xiao, Q. Zhao, X. Yang, and A. Zhu, "A Power Performance Online Assessment Method of a Wind Turbine Based on the Probabilistic Area Metric," 2020.
- [36] Y. M. Saint-Drenan, R. Besseau, M. Jansen, I. Staffell, A. Troccoli, L. Dubus, J. Schmidt, K. Gruber, S. Simões, and S. Heier, "A parametric model for wind turbine power curves incorporating environmental conditions," *Renewable Energy*, vol. 157, pp. 754–768, 2020, doi: 10.1016/j.renene.2020.04.123.
- [37] L. Lu, H. Yang, and J. Burnett, "Investigation on wind power potential on Hong Kong islands — an analysis of wind power and wind turbine characteristics," vol. 27, pp. 1–12, 2002.
- [38] V. Sohoni, S. C. Gupta, and R. K. Nema, "A Critical Review on Wind Turbine Power Curve Modelling Techniques and Their Applications in Wind Based Energy Systems," vol. 2016, no. region 4, 2016.
- [39] H. Yang, L. Lu, and W. Zhou, "A novel optimization sizing model for hybrid solar-wind power generation system," vol. 81, pp. 76–84, 2007, doi: 10.1016/j.solener.2006.06.010.
- [40] X. Liu, Y. Kang, H. Chen, and H. Lu, "Comparison of surface wind speed and wind speed profiles in the Taklimakan Desert," no. 10 m, pp. 1–18, 2022, doi: 10.7717/peerj.13001.
- [41] J. Freeman, J. Jorgenson, P. Gilman and T. Ferguson, "Reference Manual for the System Advisor Model 's Wind Power Performance Model," no. August, 2014.
- [42] A. M. M. Patnode, "Simulation and Performance Evaluation of Parabolic Trough Solar Power Plants by," 2006.
- [43] J. Wang, J. Wang, X. Bi, and X. Wang, "Performance Simulation Comparison for Parabolic Trough Solar Collectors in China," *International Journal of Photoenergy*, vol. 2016, 2016, doi: 10.1155/2016/9260943.
- [44] E. Shagdar, B. G. Lougou, B. Sereeter, Y. Shuai, and A. Mustafa, "Performance Analysis of the 50 MW Concentrating Solar Power Plant under Various Operation Conditions," *Energies*, vol. 15, no. 4, pp. 1–24, 2022, doi: 10.3390/en15041367.
- [45] M. J. Wagner, P. Gilman, M. J. Wagner, and P. Gilman, "Technical Manual for the SAM Physical Trough Model Technical Manual for the SAM Physical Trough Model," 2011.
- [46] G. Coccia, G. Latini, and M. Sotte, "Mathematical modeling of a prototype of parabolic trough solar collector Mathematical modeling of a prototype of parabolic trough solar collector," vol. 023110, no. May 2014, 2013, doi: 10.1063/1.3699620.
- [47] G. K. Manikandan, S. Iniyar, and R. Goic, "Enhancing the optical and thermal efficiency of a parabolic trough collector – A review," *Applied Energy*, vol. 235, no. August 2018, pp. 1524–1540, 2019, doi: 10.1016/j.apenergy.2018.11.048.
- [48] A. Bilal, M. N. Khan, M. Zubair, and E. Bellos, "Commercial parabolic trough CSP plants : Research trends and technological advancements," *Solar Energy*, vol. 211, no. April, pp. 1422–1458, 2020, doi: 10.1016/j.solener.2020.09.072.

- [49] H.L. Zhang; J. Baeyens; J.Degrève and G. Cacères., “Concentrated solar power plants : Review and design methodology,” vol. 22, pp. 466–481, 2013, doi: 10.1016/j.rser.2013.01.032.
- [50] J. J. Michalsky, “The Astronomical Almanac ’ S Algorithm For Approximate Solar Position (1950-2050),” no. 3, pp. 227–235, 1988.
- [51] The Wind Power Database, “The Wind Power Database,” 2023. <https://www.thewindpower.net/> (Last accessed date: 23/01/2023)
- [52] El Khchine Younes and Sriti Mohammed, “Performance evaluation of wind turbines for energy production in Morocco ’ s coastal regions,” *Results in Engineering*, vol. 10, no. February, p. 100215, 2021, doi: 10.1016/j.rineng.2021.100215.
- [53] M. Daoudi, A. Ait, S. Mou, and L. A. Naceur, “Evaluation of wind energy potential at four provinces in Morocco using two-parameter Weibull distribution function,” vol. 13, no. 2, pp. 1209–1216, 2022, doi: 10.11591/ijpeds.v13.i2.pp1209-1216.
- [54] A. A. Teyabeen, “Statistical analysis of wind speed data,” in 2015 6th International Renewable Energy Congress, IREC 2015, 2015, pp. 160–163. doi: 10.1109/IREC.2015.7110866.